Ocean Dynamics (2019) 69:1273–1285
https://doi.org/10.1007/s10236-019-01315-w

Characteristics of saw-tooth bars on the ebb-tidal deltas of the Wadden Islands

Laura Brakenhoff[1] · Gerben Ruessink[1] · Maarten van der Vegt[1]

Received: 11 January 2019 / Accepted: 9 October 2019 / Published online: 4 November 2019

Abstract
Saw-tooth bars are shore-oblique sand bars that are found along most ebb-tidal deltas of the Frisian Wadden Islands. Although they might significantly affect sediment transport pathways and volumes on the deltas, their general characteristics and dynamics are largely unknown. The main aim of this paper is to determine the typical saw-tooth bar heights, wave lengths, widths, orientations, migration rates and depths of occurrence. To this end, we analysed bathymetries from the Dutch and German Frisian Wadden Islands between 1970 and 2015. Bar heights range between 0.5 and 2 m, and wave lengths range between 300 and 900 m, with an average of 670 m, and the bar crests have a down contour orientation of approximately 25°. The bars are between 800 and 2200 m wide. Saw-tooth bars are located at depths from 3 to 12 m, depending on the slope of the area. Migration speeds of up to 112 m/year were found, using a spatial correlation method. Bar height and migration speed are positively linearly correlated, as well as bar wave length and bar width, bar height and the orientation of the depth contours and migration speed and the orientation of the area. The derived characteristics are compared to those of other bar types to evaluate hypotheses regarding the formation mechanism of the bars.

Keywords Bedforms · Shore-oblique sand bars · Sand waves · Subtidal rhythmic morphology · Tidal inlets · Coastal morphodynamics

1 Introduction

Barrier coasts make up some 10% of the world's coast line (Stutz and Pilkey 2011). They are morphologically and ecologically highly dynamic, and understanding their dynamics is therefore vital for managing purposes (Wang et al. 2012). Typically, barrier coasts consist of a series of islands, intersected by tidal inlets, with flood-tidal deltas on their landward side and ebb-tidal deltas on their seaward side (Hayes 1979, 1980). Ebb-tidal deltas are relatively shallow and can protect the adjacent islands and their back-barrier basin against high storm wave energy. Their high sediment volumes, between 1 and 100 × 10^6 m^3 (Gaudiano and Kana 2001) can serve as a sediment source for adjacent islands and the back-barrier basin, as suggested for the Dutch Wadden Sea barrier coast by Elias et al. (2012). Nonetheless, sediment transport pathways on ebb-tidal deltas are still poorly understood (Wang et al. 2012).

The effects of sediment transport on ebb-tidal deltas can be visible by bars that migrate and attach to the coast or migrating sand waves (e.g. Bruun and Gerritsen 1959). Large-scale bedforms can affect the amount of transported sediment in two ways: directly by migrating and therefore literally transporting sediment (e.g. Simons et al. 1965; Aberle et al. 2012) and also indirectly by altering the spatial flow structure (Kwoll et al. 2014). A typical example of an ebb-tidal delta showing different types of bedforms is given in Fig. 1; the bedforms are described below.

On some ebb-tidal deltas, single bars are found, which are referred to as swash bars (Hayes 1980). They are generated by waves breaking on the edges of the ebb-tidal delta, thereby reworking sand that was transported seaward through the ebb-channel (Hine 1975). These swash bars are 0.5–2.0 m high, 50–150 m long and 50 m wide (Davis and Dalrymple 2012). As visible in Fig. 1, swash bars are oriented more or less perpendicular to the shoreline. They migrate with 100–400 m/year. The migration rate of the individual bars decreases in the onshore direction because of the increasingly larger bar height (FitzGerald 1988). This leads to the formation of large bar complexes or shoals (FitzGerald 1982). FitzGerald

Responsible Editor: Birgit Andrea Klein

✉ Laura Brakenhoff
l.b.brakenhoff@uu.nl

[1] Department of Physical Geography, Faculty of Geosciences, Utrecht University, P.O. Box 80.115, 3508 TC Utrecht, The Netherlands

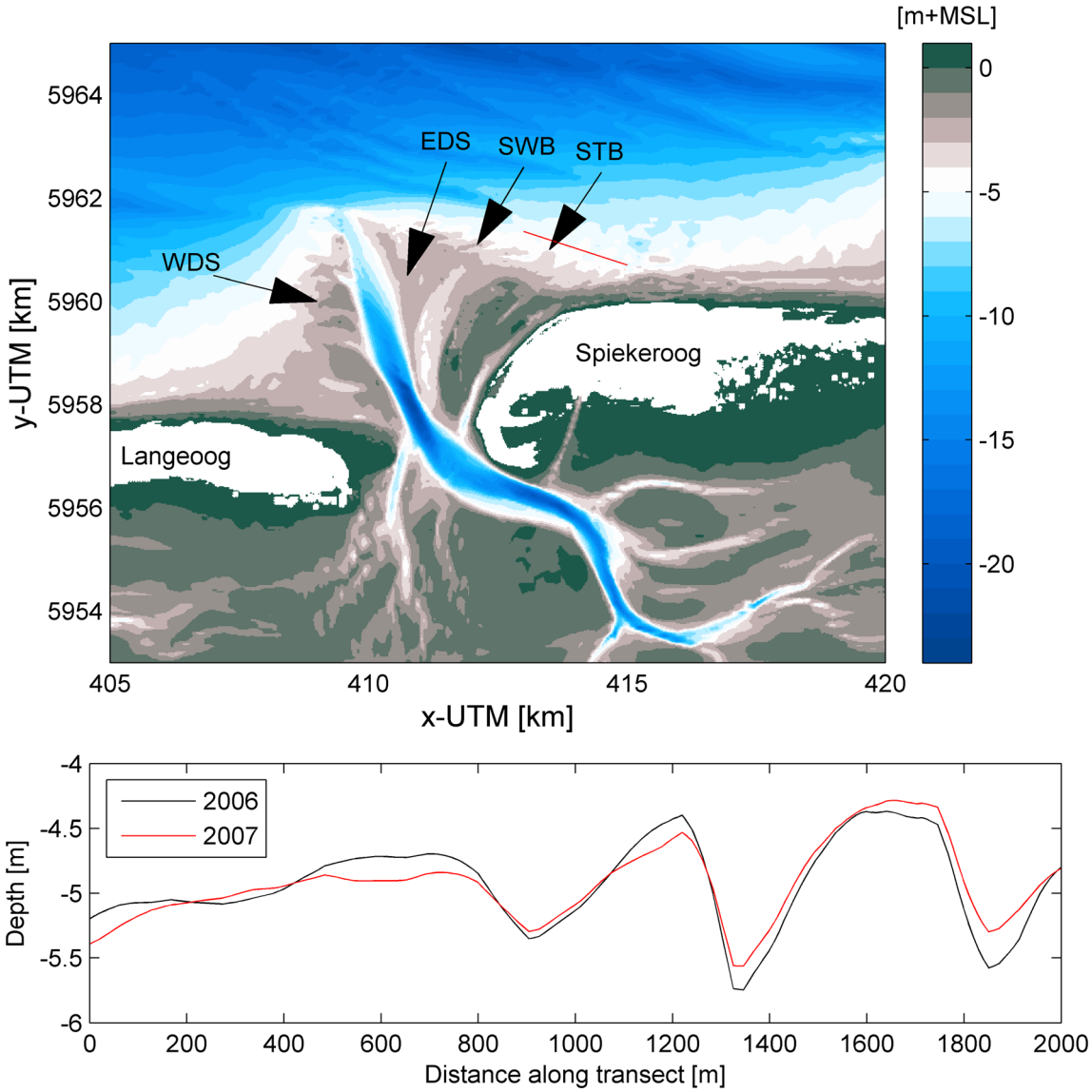

Fig. 1 Upper plot: Typical example of a Wadden Sea Inlet (Otzumer Balje Inlet, 2006) including the following bedforms: western/eastern ebb-tidal delta shoals (WDS/EDS), swash bars (SWB) and saw-tooth bars (STB). Red line indicates the transect location of the lower plot. Lower plot: cross-section along the transect in 2006 and 2007, showing some typical characteristics like height, wavelength and asymmetry of saw-tooth bars

(1988) and Gaudiano and Kana (2001) found that volumes of these shoals range between 1×10^5 and 1.5×10^6 m^3 for inlets in South Carolina, USA. Shoal migration velocities on the ebb-tidal deltas of the Wadden Sea range between 67 and 351 m/year (Ridderinkhof et al. 2016a). Shoals move onshore because landward flow by waves and tides is dominant over seaward flow consisting of only tides (Ridderinkhof et al. 2016b). They have a typical cycle of growth, migration and attachment to the downdrift island (FitzGerald 1996; Israel and Dunsbergen 1999). The periods between successive shoal attachments vary between 4 and 130 years (Ridderinkhof et al. 2016a).

In the Wadden Sea area, besides the bedforms mentioned above, saw-tooth bars (or shore-oblique sandbars or subtidal rhythmic morphology) are found on the downdrift side of the ebb-tidal delta (longshore drift is to the east). They have been given much less scientific attention, and a general understanding of their characteristics is missing. We do have results from case studies that were based on an analysis of sometimes one to maximum three bathymetries of single ebb-tidal deltas, but a systematic overview based on an analysis of all available bathymetries along the Wadden Sea is missing. The first description of saw-tooth bars was given by Reineck (1963), who studied the shoreface of Norderney in 1961. He found that the downdrift side of saw-tooth bars is steeper than the upstream side and therefore named them saw-tooth bars. Yet, no other accounts of their asymmetry are known other than that of Gordeau (1999), who found that the crests and troughs are

of approximately equal width. In general, saw-tooth bar heights are 0.5–3 m (Reineck 1963; Gordeau 1999; Brakenhoff et al. 2017). Wave lengths are in between 400 and 1200 m, with large differences between inlets (Reineck 1963; Antia 1994, 1996; Gordeau 1999). Reineck (1963) and Gordeau (1999) showed that the cross-shore bar widths are larger than the wavelengths; widths range from 500 to 2000 m. Antia (1994, 1996) showed that saw-tooth bars originate in a water depth of 2–6 m. In contrast to the swash bars, saw-tooth bars bars are shore-oblique and current-transverse but tend to become more shore-normal in the easterly (downdrift) direction (Reineck 1963; Antia 1994). Figures in Antia (1994) show that the saw-tooth bars originate on the part of the ebb-tidal delta that is downdrift of the dominant longshore drift direction, but it is still unknown how these bars are generated. Saw-tooth bars tend to migrate. Yet, Antia (1994) states that migration is rotational around nodal points, while Gordeau (1999), Elias (2006) and Herrling and Winter (2014) found translational migration in the direction of the littoral sediment drift in the order of 100–200 m/year. Also, volumetric transport rates were estimated to be in the order of 10^5 m^3/year, assuming that the unknown constant factor is zero (Brakenhoff et al. 2017).

In short, all knowledge on saw-tooth bars is based on a few case studies, and a more systematic overview of their characteristics is missing. The main aim of this paper is to determine the characteristics of saw-tooth bars based on an analysis of bathymetries of all ebb-tidal deltas of the Wadden Sea region. In Sect. 2, the available data and data analysis methods are described. Section 3 gives an overview of the various characteristics that were studied, as well as the relations between those characteristics. Furthermore, we will relate saw-tooth bar characteristics to the orientation and slope of the shoreface and the tidal range. In Sect. 4, the characteristics as found in the present study will be compared to those found in literature, and they will be used to evaluate hypotheses regarding saw-tooth bar formation. The conclusions are provided in Sect. 5.

2 Methods

2.1 Study area

The study area is the Wadden Sea, which stretches from the north of the Netherlands to the west of Denmark. Because saw-tooth bars were not observed in Denmark, we focus on the area of the West and East Frisian Islands (Fig. 2). This area can be classified as mixed energy tide-dominated to wave-dominated, depending on location. All inlets have well-developed ebb-tidal deltas (Elias et al. 2012). Mean significant wave height is 1.3 m, but wave heights can become up to 6 m during storms. The tidal wave propagates from west to east, with the tidal range increasing from 1.4 m near the Texel Inlet to 3 m near the Harle Inlet (Elias et al. 2012; Balke et al. 2016).

2.2 Available data

Since 1990, the bathymetries of the Dutch ebb-tidal deltas have been measured every 3 to 6 years by Rijkswaterstaat (part of the Dutch Ministry of Infrastructure and the Environment); see Table 1. Since 2005, the Ameland Inlet and ebb-tidal delta have been measured almost every year. Before 1990, measurements occurred more sporadically. Until the 1960s, data were recorded manually and after that with a single-beam echosounder on arrays perpendicular to the shore with 200 m spacing. They were linearly interpolated and stored on a 20 × 20-m grid with an estimated depth accuracy of 0.11 to 0.40 m (Perluka et al. 2006).

In Germany, bathymetric surveys were performed by various institutes between 1982 and 2012, and these were collected by the Bundesamt für Seeschiffart und Hydrographie (BSH). The bathymetries are stored in regular 50 × 50-m grids and are composed of data that were interpolated in space and time (Valerius et al. 2013). The depths were originally measured at irregular spatial and temporal intervals, but in the dataset, the uncertainties are provided for all grid cells in space and time. Data were not used if the uncertainty on the depth was larger than 2 m (due to interpolation in space and time), or when they were interpolated in time. The average depth accuracy of the German survey data used here was 0.83 m.

The inlets where saw-tooth bars are found are indicated in Fig. 2, and the years in which bathymetries are measured for those inlets are presented in Table 1. All x and y coordinates are given in UTM, and all depth values are given in m with respect to mean sea level (MSL).

2.3 Data analysis

An example of a measured bathymetry (Ameland Inlet 2005) is shown in Fig. 3a. Although saw-tooth bars are already visible, to better see the bed forms, a spatial running mean with an area of 1000 × 1000 m was calculated around each grid point in each bathymetry (Fig. 3b). Subsequently, this running mean was subtracted from the actual bathymetry (Fig. 3a), revealing the bedforms as perturbations from the mean (Fig. 3c). On such a perturbation map, the area with saw-tooth bars occur was indicated manually (further referred to as bar area). An example of a bar area is given in Fig. 3c. Saw-tooth bars were classified as such if (1) they are located on the downdrift side of the ebb-tidal delta, (2) more than 1 bar is visible, (3) the bar width (i.e. shore-normal bar crest length) is larger than their wavelength, (4) their height is at least 0.5 m (larger than the measurement uncertainty) and (5) they are not

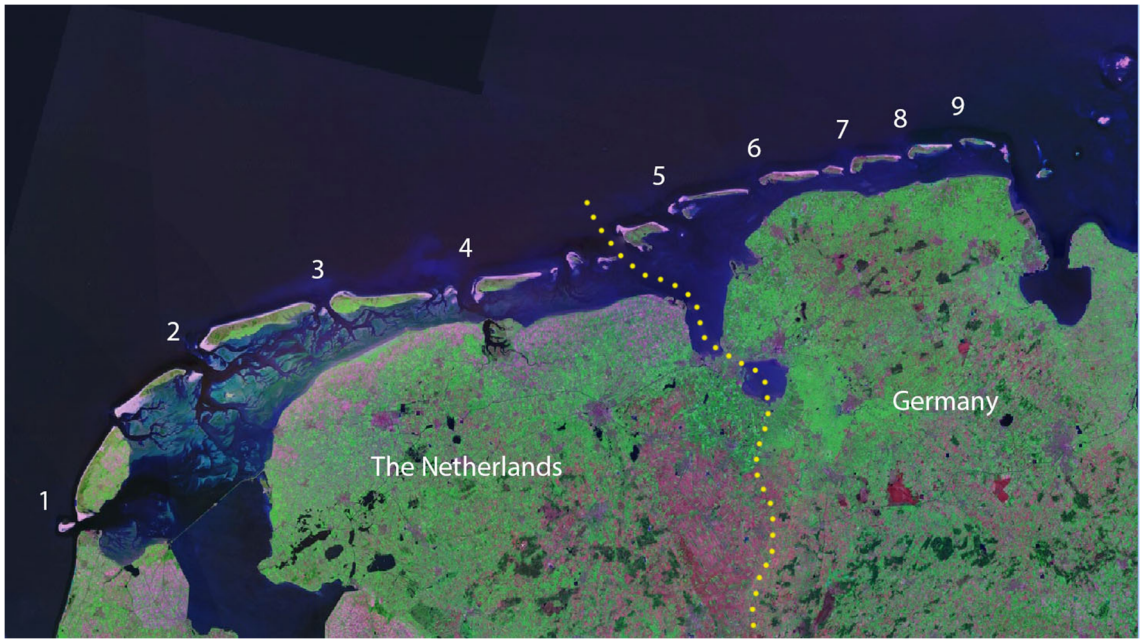

Fig. 2 The West and East Frisian Wadden Islands (border in yellow dots). Numbers denote the inlets with saw-tooth bars. 1 Texel Inlet, 2 Vlie Inlet, 3 Ameland Inlet, 4 Frisian Inlet, 5 Osterems, 6 Norderneyer Seegat, 7 Accumer Ee, 8 Otzumer Balje Inlet, 9 Harle Inlet (Source: NASA)

oriented parallel to the downdrift shoreline (that would imply that they are swash bars or surf zone bars).

The bar width and depths of occurrence were determined manually for all available bathymetries. First, the two ends of each bar crest were selected in the perturbation plot (Fig. 3c). After that, the distance between them was calculated and the accompanying depths in the mean bathymetry (Fig. 3b) were determined.

Following Smith (1997), the bar height (crest to trough) was calculated by multiplying the standard deviation of the perturbations around the mean in the bar area by a constant, which depends on the shape of the bars (square, triangle or sine waves). In general, saw-tooth bars have the closest resemblance to sine waves, so the bar height was calculated by $2{\cdot}\sqrt{2}{\cdot}s$, with s being the standard deviation within the bar area.

To verify that the bars are actually symmetric, the asymmetry (AS) was calculated. AS is given by the distance from trough to crest, divided by the distance from crest to crest. With this calculation, values are always in between 0 and 1, and the bar is fully symmetric if AS = 0.5. If the bars are asymmetric, a value between 0.5 and 1 is to be expected; this would indicate a downdrift directed bar.

Bar wave length and crest orientation were deduced from a 2D Fast Fourier Transformation (FFT) of the bar area in the perturbation plot (Fig. 3d). The FFT is used to calculate the bar wave length and orientation of the saw-tooth bars with respect to the north. For this, the spatial frequency k (inverse wavelength) was first calculated as $k = \sqrt{{k_{x,max}}^2 + {k_{y,max}}^2}$. In this equation, $k_{x,max}$ and $k_{y,max}$ are the x and y location of the maximum intensity in the FFT plot (Fig. 3d). Wavelength L was then determined as $L = 1/k$. Orientation θ is given by $\theta = \tan^{-1}(k_{y,\,max}/k_{x,\,max}) - 90$ (Fig. 3c). However, since the orientation of the ebb-tidal deltas and coastlines of the various

Table 1 Available bathymetries

Inlet	Years with bathymetry available
1. Texel Inlet	1926, 1948, 1971, 1981, 1986, 1991, 1994, 1997, 1999, 2001, 2006, 2009, 2012, 2015
2. Vlie Inlet	1971, 1975, 1981, 1988, 1992, 1995, 1998, 2000, 2002, 2004, 2007, 2010, 2013, 2016
3. Ameland Inlet	1975, 1989, 1993, 1996, 1999, 2002, 2005, 2006, 2007, 2008, 2010, 2011, 2012, 2014, 2016, 2017
4. Frisian Inlet	1927, 1949, 1958, 1970, 1975, 1979, 1982, 1987, 1991, 1994, 1997, 2000, 2002, 2005, 2009, 2012, 2015
5. Osterems	1985, 1986, 1989, 1990, 1995, 1996, 1998, 1999, 2000, 2001, 2002, 2003, 2004, 2005, 2006, 2007, 2008, 2009, 2010, 2011
6. Norderneyer Seegat	1986, 1987, 1989, 1990, 1992, 1993, 1995, 1996, 1998, 1999, 2001, 2002, 2004, 2005, 2006, 2007, 2008, 2009, 2010, 2011
7. Accumer Ee	1985, 1986, 1989, 1990, 1992, 1993, 1995, 1996, 1998, 1999, 2000, 2001, 2002, 2004, 2005, 2006, 2007, 2008, 2009
8. Otzumer Balje Inlet	1985, 1986, 1989, 1992, 1993, 1995, 1996, 2001, 2002, 2004, 2005, 2006, 2007, 2008, 2009, 2011, 2012
9. Harle Inlet	1992, 1993, 1995, 1996, 1997, 1998, 1999, 2000, 2001, 2002, 2003, 2004, 2005, 2006, 2007

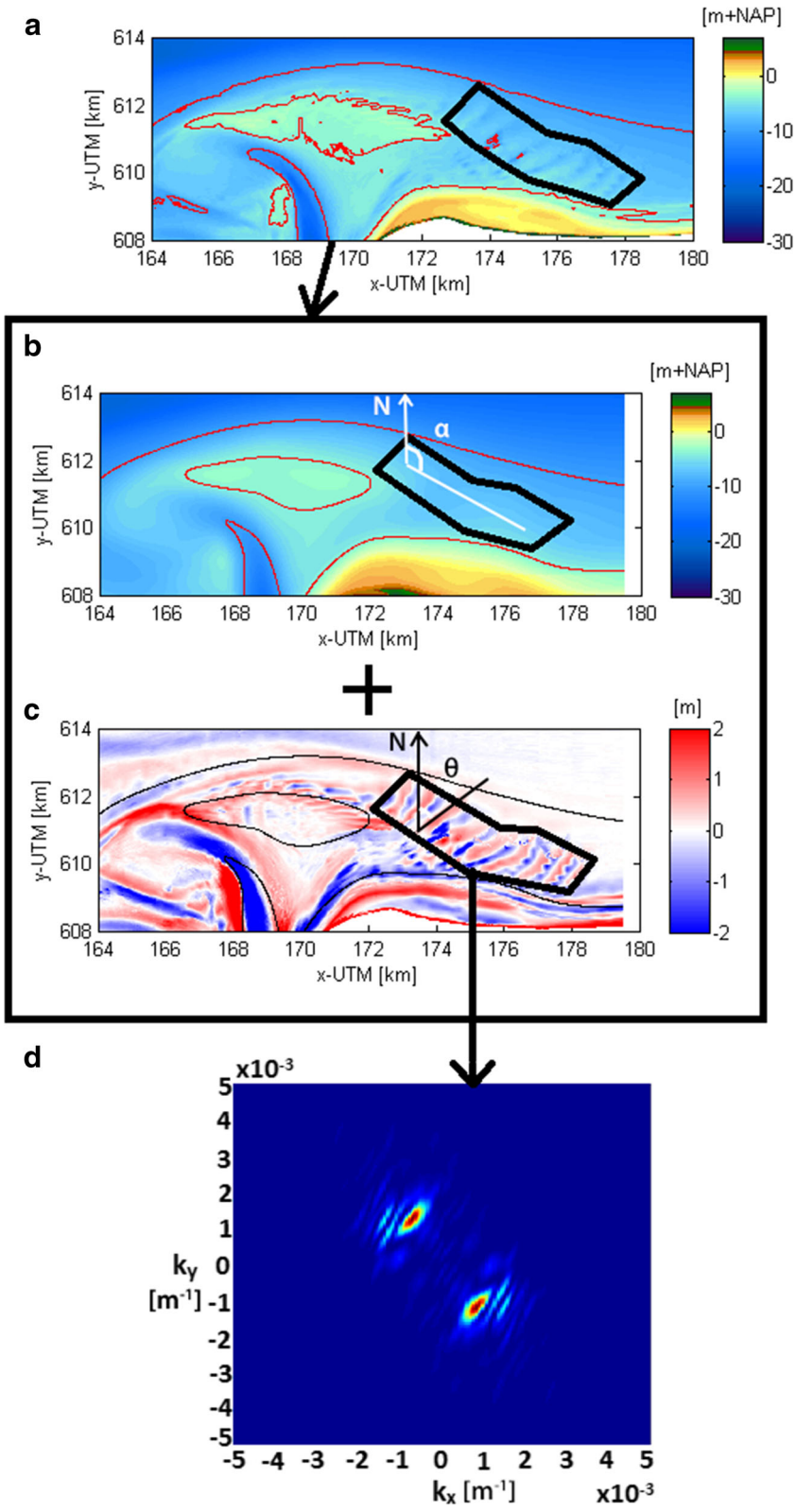

Fig. 3 Calculation of the various bar characteristics. **a** The original bathymetry (Ameland Inlet, 2005), with 4- and 10-m depth contours in red. **b** The mean bathymetry, with 4- and 10-m depth contours in red and the definition of the orientation of the depth contours in white. **c** Perturbation bathymetry, with the black angle indicating the orientation of the bars. **d** FFT of the bar area. **b** is used for the calculation of the slope and orientation of the area α and the depth of bar occurrence. **c** is used for the calculation of bar height and width. **d** is used to calculate bar wave length and orientation θ.

islands differs, these orientations cannot be compared to each other. Therefore, the orientation of the saw-tooth bar area was calculated as well. This was done by fitting a linear surface through the mean bathymetry of the bar area and subsequently determining the average bed slope and the orientation. The orientation of the area α was defined as the average angle between the depth contours of the linear surface and the North (Fig. 3b).

The migration speeds of the saw-tooth bars were derived from spatial correlation of two perturbation maps of the bar area at subsequent moments in time. The method of Duffy and Hughes-Clarke (2005) was used. First, a search area was defined, which typically contained one saw-tooth bar. Therefore, in the present study, the search area was chosen to be 600 × 600 m. Within the search area, a square matrix was created around each grid point, called the fit matrix ($f(x,y)$ at time T1). The size of the fit matrix was 200 × 200 m. Next, a displacement matrix (r) was determined, consisting of the correlation between $f(x,y)$ and a displaced fit matrix of a subsequent year T2 for each possible displacement within the search area ($g(x + \Delta x, y + \Delta y)$). The result is a matrix of correlation values $r_{k,l}$ on each location (x,y):

$$r_{k,l}(x,y) = \sum_{k=0}^{kmax} \sum_{l=0}^{lmax} f(x,y) g(x + \Delta x_k, y + \Delta y_l). \quad (1)$$

To prevent biases due to potential outliers, the correlation r was normalized by subtracting the mean from each dataset, and subsequently dividing by the standard deviation. From now on, the correlation was called R. Values in R lower than 0.3 were removed, because they indicate a low to insignificant correlation. In the resulting R matrix, the migration correlation was determined as the weighted centroid of all $R > R_{max}/\sqrt{2}$. The migration of the fit matrix is given as the distance between the centre of the fit matrix and the location of the migration correlation. The total migration of the saw-tooth bar field is the average of all fit matrix migration values.

The calculation of migration speed was only possible when the two bathymetries were taken within 1 or 2 years from each other. When there is more time between two bathymetries, either the shape of the bars changes too much or the bars migrate more than one wavelength. Therefore, the migration speed was not computed for the saw-tooth bars at the Texel, Vlie and Frisian Inlets.

3 Results

The relations between all studied variables, based on a linear regression, can be found in Tables 2 and 3. All variables will now be described separately.

3.1 Bar height and asymmetry

The height of the saw-tooth bars is between 0.5 and 2 m (Fig. 4), although for the German inlets (Osterems until Harle Inlet) it is more commonly between 0.5 and 1 m. The largest bar height is 2.27 m, which was found for 2006 on the ebb-tidal delta of the Ameland Inlet. Both median and maximum bar heights decrease from Ameland to the east. Along each individual ebb-tidal delta, the bar heights are more or less constant in space.

On most ebb-tidal deltas, the bar heights were found to vary in time, but the time scales involved varied at and between locations. Overall, the largest time scales were found at the Dutch inlets. As an example, the bar height at the Ameland Inlet first increased from less than 0.5 to 2.27 m in about 15 years, and then decreased again to less than 0.5 m in about 10 years (Fig. 4a). Other systems show similar behaviour. The peaks in bar height occur simultaneously at the Texel, Vlie and Frisian inlets, but no relation can be found with the peak bar height at the other inlets. For the German inlets, the absolute bar height variations in time are small, and at several moments, no bars were found at all. This was the case in the Accumer Ee Inlet in 1987 and in the Harle Inlet in 1987, 1988, 2002, 2003 and 2006 (Fig. 4c). After their disappearance, they can reappear within a few years. These observations will be further addressed in the discussion.

Bar heights are linearly correlated to the slope and orientation of the area. The correlation is negative between bar height and the slope of the area, meaning that the bar height decreases for steeper shorefaces. The correlation between bar height and area orientation is positive, meaning that the bars are higher when the depth contours are deflecting more away from the north.

The asymmetry of the saw-tooth bars is approximately constant in space and time. On average, the asymmetry is 0.53, which indicates that the assumption of symmetric bars was correct, and thus proving that saw-tooth bars are actually very symmetric. The standard deviation is 0.13, indicating that the spread is indeed low.

3.2 Bar wave length and orientation

Figure 5 shows the distribution of wave lengths per tidal inlet system. The values range between 313 and 909 m, with an overall average of 672 m. The smallest median wavelengths (400 m) are found for the westernmost inlet (the Texel inlet), whereas the largest median wavelengths (830 m) are found in the next (Vlie) inlet. From there on, the median wavelength decreases in eastward direction to 500 m. This observation will be further addressed in the Sect. 4.

Analogous to the bar heights, the bar wavelengths also fluctuate on a multi-annual timescale. Time scales are similar to those of the bar heights, but peak heights and lengths do not occur simultaneously. Again, the timescales associated with wavelengths on the German ebb-tidal deltas are shorter, more in the order of years. On the other hand, the range in wavelengths, as given by the interquartile range, is larger for the German inlets (Fig. 5).

Figure 6 presents the orientation of the bars with respect to the mean orientation of the bar area, showing that the bar orientation is similar for all inlets. On average, the

Table 2 Values of the linear coefficient of correlation (r) for all combinations of sandbar characteristics. Italicized values have $p < 0.01$

	Bar height	Wavelength	Orientation	Width	Landward depth	Seaward depth	Asymmetry	Migration
Migration	*0.47*	0.19	− 0.19	− 0.03	− 0.20	0.04	0.49	
Asymmetry	0.22	0.28	− 0.10	0.09	0.12	− 0.04		
Seaward depth	− 0.17	*− 0.57*	*− 0.19*	*− 0.83*	*0.79*			
Landward depth	*− 0.28*	*− 0.47*	− 0.04	*− 0.58*				
Width	0.21	*0.45*	*0.21*					
Orientation	− 0.13	*− 0.22*						
Wavelength	0.17							
Bar height								

angle between the bar crests and the underlying depth contours is 66°, meaning that the bar crests have a slight down contour orientation of 25°. No changes with time were found.

No significant relation was found between the orientation of the bars and the bar height. The bar wavelength, on the other hand, seems to decrease for increasing bar angles (Table 2). Wavelength and bar orientation are not correlated to the slope and orientation of the area (Table 3).

3.3 Bar width

Figure 7 shows that the bar widths are generally between 670 and 2500 m. The widths increase from west to east in the Dutch inlets, whereas in the German inlets, widths decrease from west to east. The widths vary on a time scale similar to the lengths and heights, but peaks do not coincide. They are negatively correlated to the bed slope and orientation (Table 3), meaning that the bar width is smaller when the shoreface is steeper or more oblique. On top of that, bars with larger wavelengths also have larger widths (Table 2). The ratio width/wave length is in between 1.5 and 3.5 for all inlets, with the higher values for the Texel, Frisian and Osterems Inlet, and the lower values for the other inlets.

3.4 Depths of occurrence

Depths of the landward ends of the bars range between 3 and 8 m while depths of the most seaward end of the bars are in between 5 and 12 m (Fig. 8). The largest interannual variability in nearshore and seaward depths is found in the German inlets, which is visible in the amount of scatter in Fig. 8. For example, the seaward depths of the Osterems ranges between 9.5 and 12 m, while those of the Ameland Inlet range between 7.5 and 9 m.

Bars that start deeper also end deeper and vice versa. Seaward and landward depth are positively correlated (Table 2). Besides the relation between the landward and seaward depth, these depths and the slope of the shoreface are also negatively correlated (Table 3). When the shoreface is steeper, the most landward end of the bars is found on shallower depths. The same holds for the seaward depth. The depths of occurrence also have a relation with the bar wave length; bars that occur on larger depths are longer. This is true for both landward and seaward depth (Table 2). Naturally, bars that are wider also extend to deeper areas. Yet, it was also found that wider bars also tend to start at larger depths.

3.5 Migration speed

The migration speed of the saw-tooth bars for all inlets varies between 2 and 112 m/year (Fig. 9). On average, the bars migrate with 30 m/year, but it is visible that the migration speed highly depends on the location of the inlet along the Wadden Sea coast. At the Norderneyer Seegat and the Accumer Ee Inlet, migration speeds are very low, while at the same time, the bars move quite fast at the Ameland and Harle Inlet. Apart from their relation with their position along the Wadden coast, bars with larger heights tend to migrate faster than lower bars (Table 2). Both characteristics fluctuate on similar multi-annual timescales. On top of that, migration is positively correlated to the orientation of the shoreface (Table 3).

Table 3 Values of the linear coefficient of correlation (r) between bar area and sandbar characteristics. Italicized values have $p < 0.01$

	Bar height	Wavelength	Orientation	Width	Landward depth	Seaward depth	Asymmetry	Migration
Area slope	*0.28*	0.05	0.12	*0.52*	*− 0.44*	*− 0.38*	0	0.05
Area angle	*0.27*	− 0.21	0.04	*− 0.34*	0.20	0.35	0.06	*0.46*

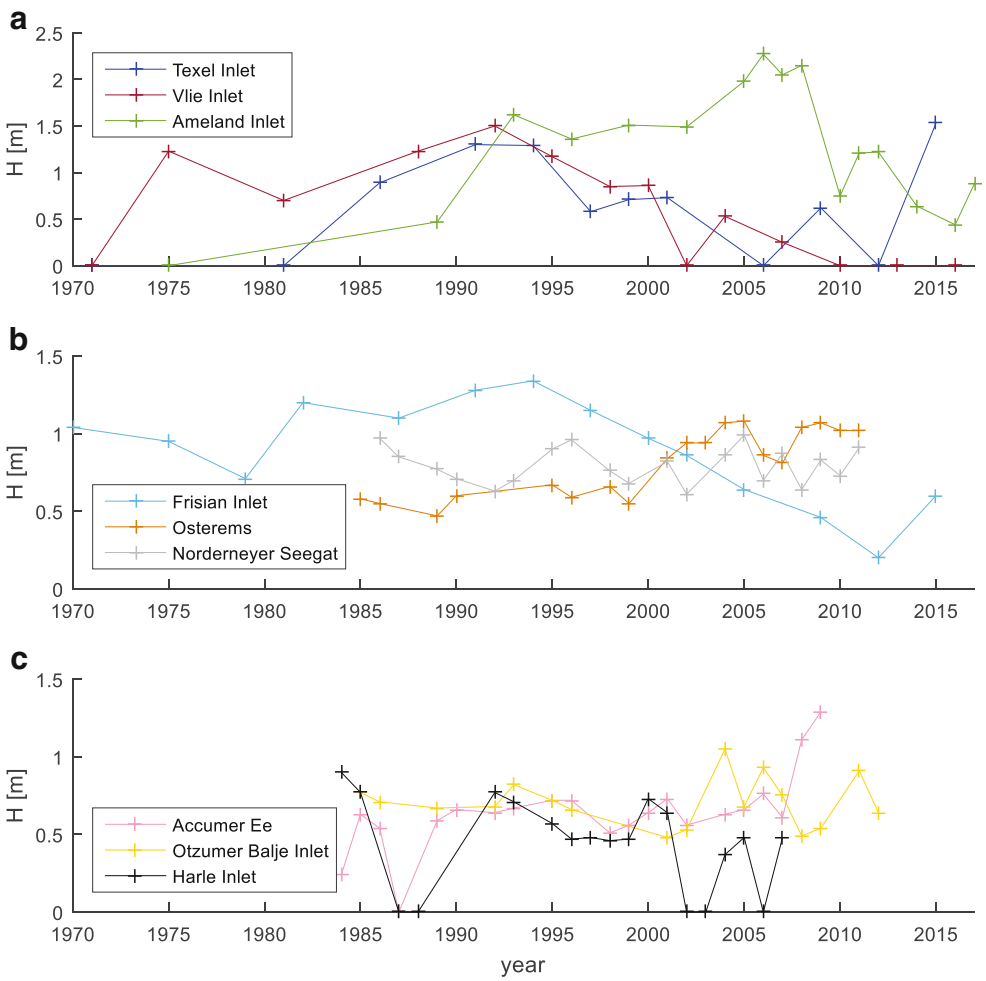

Fig. 4 Absolute height of the saw-tooth bars for all inlets through time

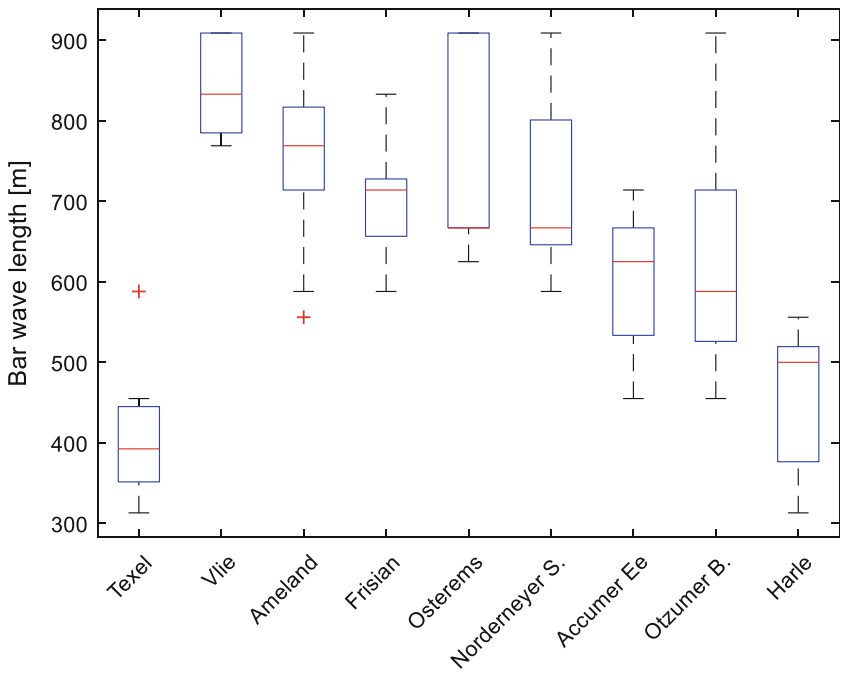

Fig. 5 Occurrence of alongshore saw-tooth bar lengths. The red line in each box indicates the median, and the bottom and top edges of the box indicate the 25th and 75th percentiles, respectively. The whiskers extend to the most extreme data points not considered outliers, and the outliers (more than 1.5 times the interquartile range away from the top or bottom of the box) are plotted using the '+' symbol

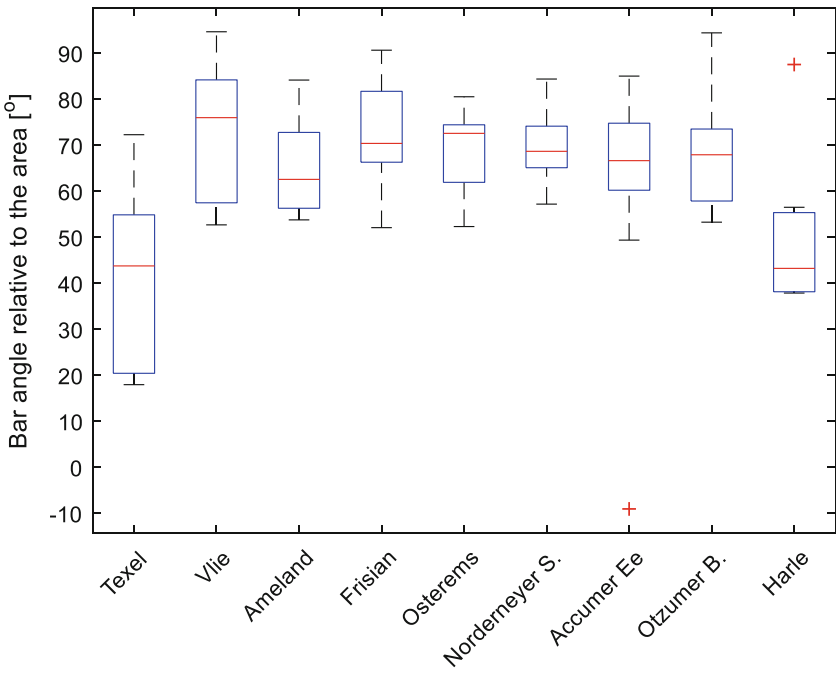

Fig. 6 Occurrence of the angle between the bar crests and the bar area. Symbols are explained in Fig. 5

4 Discussion

In this study, the characteristics of saw-tooth bars were analysed and combined into a complete and systematic overview. The found characteristics were within the range as found in previous studies, but the present study is the first to enable determining spatial trends, temporal behaviour and relations between the bar characteristics and their environment. Yet, it is still unclear how their characteristics compare to other bar types found on continental shelves and by which mechanisms they are generated. These two questions will be discussed below.

4.1 Saw-tooth bar properties compared to other bar types

Antia (1994) classified saw-tooth bars as surf zone transverse bars, but the findings of this paper indicate that they are not. Like saw-tooth bars, transverse bars are oriented perpendicular or oblique to the shore and are 0.3–2 m high (e.g. Ribas et al. 2015). However, they are typically found in wave-dominated surf zones (e.g. Wright and Short 1984). Yet, the longest type of transverse bars, the transverse bar and rip (TBR), has a wavelength of 75–750 m and a width in the order

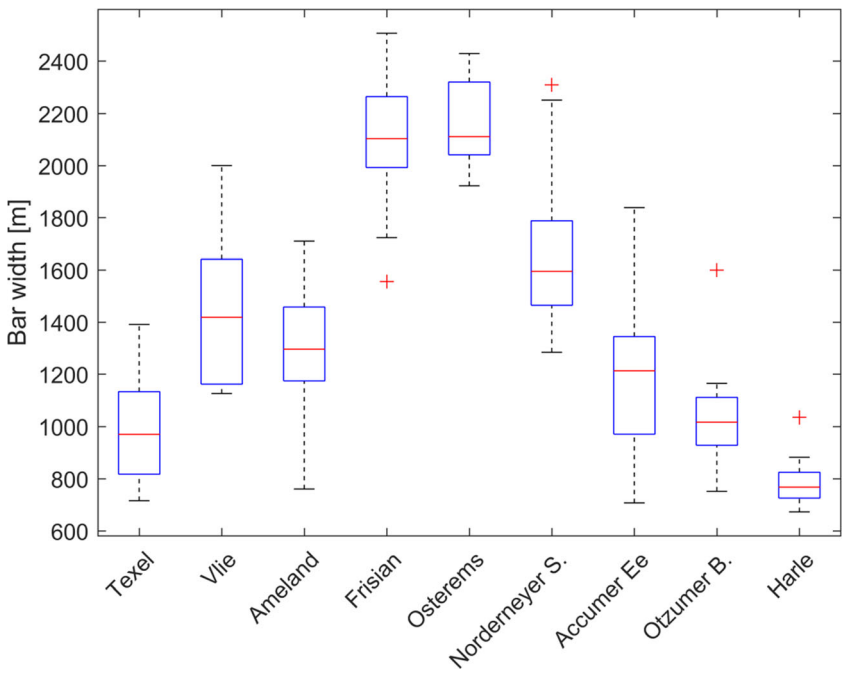

Fig. 7 Bar crest length for all inlets. Symbols are explained in Fig. 5

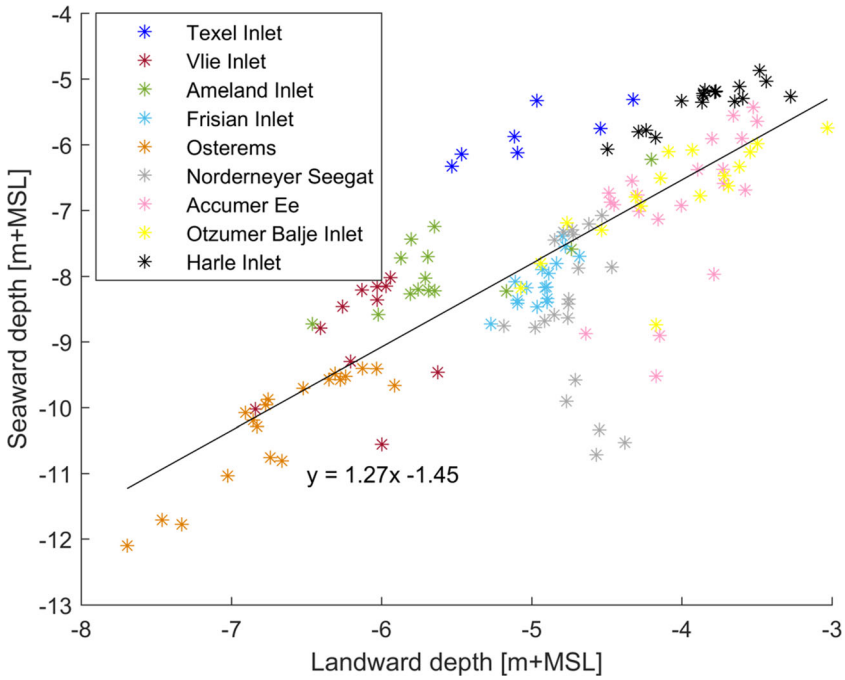

Fig. 8 Relation between nearshore and offshore depth

of 100 m. Other transverse bars (large-scale finger bars, LFB) were found in the low-energy microtidal environment of Florida (USA) by Gelfenbaum and Brooks (2003). The main similarities between LFB and saw-tooth bars are their height, and the fact that both types of bars reach out of the surf zone. However, LFB have wavelengths of approximately 100 m and widths of up to 4 km. Saw-tooth bars, on the other hand, always have wavelengths of at least 300 m and widths in the order of 800–2200 m. While the maximum depth at which saw-tooth bars are found is 12 m, for LFB, this is approximately 8 m. This, in combination with the high-energy macrotidal environment of the Wadden Sea, suggests that the processes acting on saw-tooth bars are probably different from those acting on LFB.

Another bar type with similarities to saw-tooth bars is the shoreface connected sand ridge (SCR) (Swift et al. 1978; De Swart and Calvete 2003). They also occur on depths of 5–20 m. SCR are several meters high, and much larger than saw-tooth bars: widths are in the order of 10 km and wave lengths in the order of 5 km (Swift

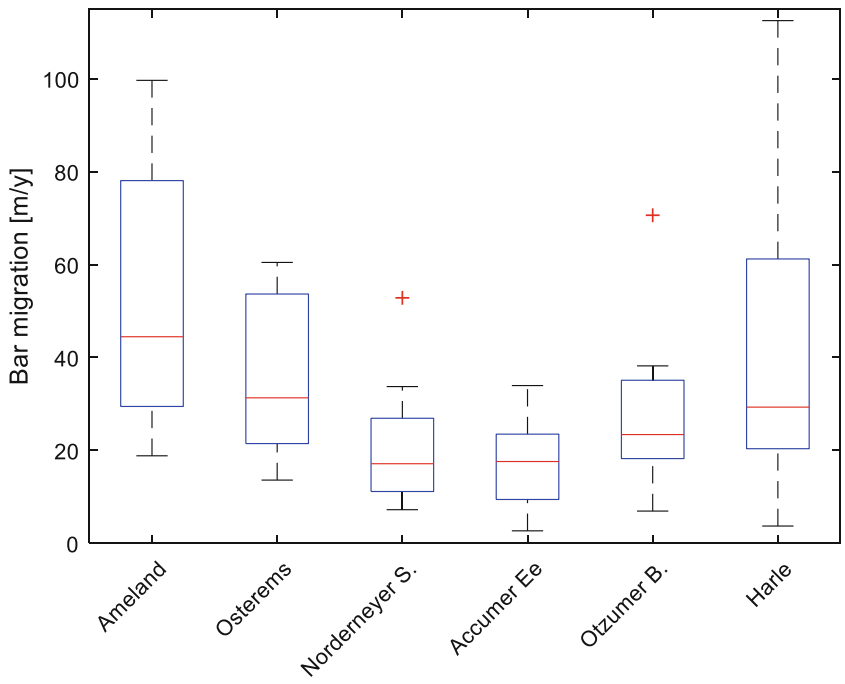

Fig. 9 Migration speed of saw-tooth bars. Symbols are explained in Fig. 5

et al. 1978; De Swart and Calvete 2003). Migration on the other hand is much smaller: only several meters per year, and only by storm-induced currents (De Swart and Calvete 2003). Another difference is their orientation: while saw-tooth bars have a slight down-contour orientation (the angle between the bar crests and the depth contours is smaller than 90°), SCR are up-contour oriented (the angle between the bar crests and the depth contours is larger than 90°) (Swift et al. 1978).

Lastly, saw-tooth bars have a resemblance to sand waves (Németh et al. 2002; Besio et al. 2006; Blondeaux and Vittori 2011). Saw-tooth bars and sand waves have similar wave length scales, but sand waves occur on larger depths (~ 30 m) and their heights can be several meters (Németh et al. 2002). Because of the small currents at these large water depths, migration speeds of sand waves are in the order of only a few meters per year (Németh et al. 2002). In tidal channels, sand wave migration rates are 20–80 m/year, which is equal to the migration rates found in the present study (Buijsman and Ridderinkhof 2008). Time scales of formation and growth are more than 20 years for sand waves (Knaapen et al. 2006), while the present study found that saw-tooth bars can form 2–5 years. Sand waves are oriented more or less perpendicular to the tidal current, with a maximum counter clockwise deviation of 10° (Hulscher 1996). Hulscher (1996) further found that sand wave height increases in offshore direction, so that would explain why saw-tooth bars are lower. Sand waves are created by an instability of a sandy bed interacting with the tidal current (Besio et al. 2006; Blondeaux and Vittori 2011). Therefore, saw-tooth bars might be shallow water sand waves occurring on ebb-tidal delta lobes.

4.2 Hypotheses regarding saw-tooth bar formation

The results of this study are in agreement with Gordeau (1999) and Herrling and Winter (2014), in finding a translational migration of the bars in the direction of littoral sediment drift. However, it was also confirmed that the bars on several ebb-tidal deltas of the East Frisian islands show little to no migration, as found by Antia (1994). Antia (1994) suggested that the troughs of the saw-tooth bars were formed by rip currents resulting from edge waves. This hypothesis is an example of the so-called forcing template theory, which assumes a fixed flow pattern that would result in a fixed bedform pattern. Since then, the self-organisation theory was further developed, which has provided a better explanation for the generation and occurrence of nearshore bedforms (Coco and Murray 2007). The main reason for this is the fact that the forcing template theory does not account for the feedback and interactions between hydrodynamics and morphodynamics. On top of that, oblique wave incidence angles (which are found on most ebb-tidal deltas) cause edge waves to be progressive, which in turn causes a non-stationary flow pattern that moves downdrift much faster than the bars (Ribas et al. 2015). Lastly, flow velocities of edge waves are not large enough to significantly change the morphology (Bryan and Bowen 1998). In the light of these findings, it is more likely edge waves or rip currents—if present—are an effect of the bar morphology, rather than its cause. The formation of the bars is hypothesised to be a result of an instability mechanism caused by the interaction between the sandy bed and the hydrodynamics.

The main reason for this hypothesis is the cyclic behaviour of the bar height and their observed migration. The linear relations between bar height and migration speed and between bar height and the orientation of the larger area including the shoal suggest that the cyclic behaviour of the shoals plays an important role in the development of saw-tooth bars. Since there are clear stages of saw-tooth bar growth and disappearance, the development of saw-tooth bars is hypothesised to be similar to that of sand waves: an instability mechanism related to tidal and wave-driven currents.

There are three types of hydrodynamics that can interact with the bed and thereby generate bedforms: tides, wind- and wave-driven currents. Wind-driven currents are known to create SCR. However, as described above, SCRs have much larger dimensions than saw-tooth bars and are orientated differently with respect to the depth contours. Also, the peaks in saw-tooth bar height do not occur simultaneously at the different deltas, implying that they are not related to storminess or yearly averaged wave height, since these characteristics should be more or less similar throughout the study area. Therefore, it is unlikely that saw-tooth bars are formed by wind-driven currents.

The decrease in median wavelength and bar height in the easterly direction could indicate a relation with the tide, since the tidal amplitude increases over the same distance. The smallest wavelengths occur under the largest tidal currents; this is also found for sand waves (Van Santen et al. 2011). However, the increase of the tidal amplitude does not necessarily cause an increase in tidal current velocity, since the tide is a standing wave. On top of that, the tide cannot explain the cyclicity in the bar heights.

Since wave directions are relatively constant in the study area, the effect of wave-related currents is mainly dependent on their direction with respect to the bars. Because of the cyclic behaviour of the ebb-tidal deltas, the orientation of the depth contours changes through time. A positive linear relation was found between bar height and the orientation of the bar area. A larger orientation angle of the depth contours with respect to the north indicates that the shoal is protruding further into the sea. At

this part in the cycle, the shoal creates a shadow zone in its downdrift part, where wave incidence angles are large and the waves propagate more or less parallel to the depth contours. Here, saw-tooth bars might develop. When the shoal has just attached to the coast, the depth contours and the direction of wave propagation are no longer aligned, causing the saw-tooth bars to disappear.

Also, the larger ebb-tidal deltas have the highest saw-tooth bars. Larger deltas have a larger shadow zone, so the bars have more space to develop. Out of the shadow zone, along the island coast, the bars gradually disappear. This is probably caused by the increasing angle between the direction of wave propagation and the depth contours at these locations. These observations related to the waves suggest that high-angle wave instabilities might generate saw-tooth bars (Ashton and Murray 2006). Although it is also possible that morphologic parameters of the shoreface are important as well (e.g. composition of the subsurface, types of sediment available, or slope of the shoreface), this could also explain why no saw-tooth bars are found on the N-W oriented Wadden Islands of Germany and Denmark. Further research should be done on the interaction of the bars with the hydrodynamics, and their effect on sediment transport. Since observations are limited, this should be done by a modelling study. Such studies could reveal the underlying morphodynamic instability mechanism that causes the formation of these saw-tooth bars.

5 Conclusions

Saw-tooth bars were studied using bathymetric maps of the ebb-tidal deltas of the Frisian Wadden Islands. Saw-tooth bars are down-current-oriented sandbars at the downdrift part of ebb-tidal deltas. Contrary to what their name suggests, they are not highly asymmetric. The heights of saw-tooth bars are in between 0.5 and 2 m and are varying through time with a multi-annual variability. Their wavelengths range between 300 and 900 m, with an average of 670 m, and crest lengths between 800 and 2200 m are found on the ebb-tidal deltas of the west- and east Frisian Wadden Islands. They occur between 3 and 12 m depth. Migration speeds vary between 2 and 112 m/year. Bar height and migration speed, wave length and width, and seaward and landward depth are positively correlated. Bar height and width both depend on the slope and orientation of the shoreface, and migration speeds only depend on the orientation of the shoreface. Not all inlets in the Wadden Sea contain saw-tooth bars, and not all saw-tooth bars migrate. Based on the present results, it is hypothesised that saw-tooth bars are sand waves, generated by an instability mechanism forced by tidal and wave-driven currents.

Acknowledgments This project is part of the program SEAWAD: "Sediment supply at the Wadden Sea ebb-tidal delta. From system knowledge to mega-nourishments". The authors thank Rijkswaterstaat and the Bundesamt für Seeschifffahrt und Hydrography formaking their bathymetric data available.

Funding information This research is supported by the Dutch Technology Foundation STW (project number 14489), which is part of the Netherlands Organisation for Scientific Research (NWO), and which is partly funded by the Ministry of Economic Affairs.

Compliance with ethical standards

Conflict of interest The authors declare that they have no conflict of interest.

References

Aberle J, Coleman SE, Nikora VI (2012) Bed load transport by bed form migration. Acta Geophys 60(6):1720–1743. https://doi.org/10.2478/s11600-012-0076-y

Antia EE (1994) Long-term and post-storm dynamic patterns of the subtidal rhythmic morphology along the East Frisian island coast, Germany. Geol Mijnb 73:1–12

Antia EE (1996) On the significance of ebb-tidal deltas to the development of the subtidal longshore-rhythmic morphology (Sägezahnriffe) along the German North Sea coast. Z Geomorph N F 40(4):477–485

Ashton AD, Murray AB (2006)High-angle wave instability and emergent shoreline shapes: 1. Modeling of sand waves, flying spits, and capes. J Geophys Res: Earth Surf 111(F4). https://doi.org/10.1029/2005JF000422

Balke T, Stock M, Jensen K, Bouma TJ, Kleyer M (2016) A global analysis of the seaward salt marsh extent: the importance of tidal range. Water Resour Res 52. https://doi.org/10.1002/2015WR018318.

Besio G, Blondeaux P, Vittori G (2006) On the formation of sand waves and sand banks. J Fluid Mech 557:1–17. https://doi.org/10.1017/S002211200600925

Blondeaux P, Vittori G (2011) The formation of tidal sand waves: fully three-dimensional versus shallow water approaches. Cont Shelf Res 31(9):990–996. https://doi.org/10.1016/j.csr.2011.03.005

Brakenhoff LB, Ruessink BG, Van der Vegt M (2017) Saw-tooth bar dynamics on the Ameland ebb-tidal delta. Proceedings Coastal Dynamics, pp 292–299

Bruun P, Gerritsen F (1959) Natural bypassing of sand at coastal inlets. Proc. ASCE, J. Waterways and Harbors Div. 85:75–108

Bryan KR, Bowen AJ (1998) Bar-trapped edge waves and longshore currents. J Geophys Res 103:867–884

Buijsman MC, Ridderinkhof H (2008) Long-term evolution of sand waves in the Marsdiep inlet. I: High-resolution observations. Cont Shelf Res 28:1190–1201. https://doi.org/10.1016/j.csr.2007.10.011

Coco G, Murray AB (2007) Patterns in the sand: from forcing templates to self-organization. Geomorphology 91:271–290. https://doi.org/10.1016/j.geomorph.2007.04.023

Davis RA Jr Dalrymple RW (eds) (2012) Principles of tidal sedimentology. https://doi.org/10.1007/978-94-007-0123-6_12, © Springer Science+Business Media B.V.

De Swart HE, Calvete D (2003) Non-linear response of shoreface-connected sand ridges to interventions. Ocean Dyn 53:270–277. https://doi.org/10.1007/s10236-003-0044-9

Duffy GP, Hughes-Clarke JE (2005) Application of spatial cross correlation to detection of migration of submarine sand dunes. J Geophys Res 110:F04S12. https://doi.org/10.1029/2004JF000192

Elias EPL (2006) Morphodynamics of Texel Inlet. PhD thesis. Delft University of Technology, the Directorate-General of Public Works and Water Management (Rijkswaterstaat-RIKZ) and WL | Delft Hydraulics. 262 pp

Elias EPL, Van der Spek AJF, Wang ZB, De Ronde J (2012) Morphodynamic development and sediment budget of the Dutch Wadden Sea over the last century. Neth J Geosci 91(3):293–310

FitzGerald DM (1982) Sediment bypassing at mixed tidal inlets. Coast Eng 1094–1118

FitzGerald DM (1988) Shoreline erosional-depositional processes associated with tidal inlets. In: Aubrey DG, Weishar L (eds) Hydrodynamics and sediment dynamics of tidal inlets, vol 29. Springer, New York, pp 186–225

FitzGerald DM (1996) Geomorphic variability and morphologic and sedimentologic controls on tidal inlets. J Coast Res 23:47–71

Gaudiano DJ, Kana TW (2001) Shoal bypassing in mixed energy inlets: geomorphic variables and empirical predictions for nine South Carolina inlets. J Coast Res 17(2):280–291

Gelfenbaum G, Brooks GR (2003) The morphology and migration of transverse bars off the west-central Florida coast. Mar Geol 200: 273–289. https://doi.org/10.1016/S0025-3227(03)00187-7

Gordeau L (1999) Saw-tooth bars defined; a case study of the Ameland inlet, Rijkswaterstaat RIKZ & Universiteit Utrecht, werkdocument RIKZ/OS-99.114x

Hayes MO (1979) Barrier island morphology as a function of tidal and wave regime. In: Leatherman SP (ed) Barrier Islands from the Gulf of Mexico to the Gulf of St. Lawrence. Academic Press, New York, pp 1–28

Hayes MO (1980) General morphology and sediment patterns in tidal inlets. Sediment Geol 26:139–156

Herrling G, Winter C (2014) Morphological and sedimentological response of a mixed-energy barrier island tidal inlet to storm and fair-weather conditions. Earth Surf Dyn 2:363–382. https://doi.org/10.5194/esurf-2-363-2014

Hine AC (1975) Bedform distribution and migration patterns on tidal deltas in the Chatham Harbor Estuary, Cape Cod, MA. In: Cronin LE (ed) Estuarine Research, vol 2. Academic Press, New York, pp 235–252

Hulscher SJMH (1996) Tidal induced large-scale regular bed form patterns in a three-dimensional shallow water model. J Geophys Res 101(C9):20 727–20 744

Israel CG, Dunsbergen DW (1999) Cyclic morphological development of the Ameland Inlet, the Netherlands. Proceedings of Symposium on River, Coastal and Estuarine Morphodynamics (Genova, Italy) 2: 705–714

Knaapen MAF, Hulscher SJMH, Tiessen MCH, Van den Berg J (2006) Using a sand wave model for optimal monitoring of a navigation depth. In: Parker G, Garcýa MH (eds) Proceedings of the 4th IAHR symposium on River, Coastal and Estuarine Morphodynamics, Urbana, Illinois, USA, Taylor & Francis, London, UK. https://doi.org/10.1201/9781439833896.ch108

Kwoll E, Becker M, Winter C (2014) With or against the tide: the influence of bed form asymmetry on the formation of macroturbulence and suspended sediment patterns. Water Resour Res 50:7800–7815. https://doi.org/10.1002/2013WR014292

Németh A, Hulscher SJMH, de Vriend HJ (2002) Modeling sand wave migration in shallow shelf seas. Cont Shelf Res 22:2795–2806

Perluka R, Wiegmann EB, Jordans RWL, Swart LMT (2006) Opnametechnieken Waddenzee. Report AGI-2006-GPMP-004 (in Dutch). Rijkswaterstaat Adviesdienst Geo Informatie en ICT, 32 pp

Reineck HE (1963) Sedimentgefüge im Bereich der südlichen Nordsee. Abh Senckenb Naturforsch Ges 505:1–138

Ribas F, Falqués A, De Swart HE, Dodd N, Garnier R, Calvete D (2015) Understanding coastal morphodynamic patterns from depth-averaged sediment concentration. Rev Geophys 53:362–410. https://doi.org/10.1002/2014RG000457

Ridderinkhof W, Hoekstra P, Van der Vegt M, De Swart HE (2016a) Cyclic behavior of sandy shoals on the ebb-tidal deltas of the Wadden Sea. Cont Shelf Res 115:14–26

Ridderinkhof W, De Swart HE, Van der Vegt M, Hoekstra P (2016b) Modeling the growth and migration of sandy shoals on ebb-tidal deltas. J Geophys Res Earth Surf 121:1351–1372. https://doi.org/10.1002/2016JF003823

Simons DB, Richardson EV, Nordin CF (1965) Bedload equation for ripples and dunes, Geological Survey Professional Paper 462-H. USGS, Washington

Smith SW (1997) The scientist and engineer's guide to digital signal processing. California Technical Publishing, San Diego ISBN: 0-9660176-3-3

Stutz ML, Pilkey OH (2011) Open-ocean barrier islands: global influence of climatic, oceanographic, and depositional settings. J Coast Res 27(2):207–222. https://doi.org/10.2112/09-1190.1

Swift DJP, Parker G, Lanfredi NW, Perillo G, Figge K (1978) Shoreface-connected sand ridges on American and European shelves: a comparison. Estuar Coast Mar Sci 7:257–273

Valerius J, Feldmann J, van Zoest M, Milbradt P, Zeiler M (2013) Documentation of morphological products from the AufMod project Functional Seabed Model, data format: Text files (CSV, XYZ). Bundesamt für Seeschiffart und Hydrographie. 11pp

Van Santen RB, De Swart HE, Van Dijk TAGP (2011) Sensitivity of tidal sand wavelength to environmental parameters: A combined data analysis and modelling approach. Cont Shelf Res 31(9):966–978. https://doi.org/10.1016/j.csr.2011.03.003

Wang ZB, Hoekstra P, Burchard H, Ridderinkhof H, De Swart HE, Stive MJF (2012) Morphodynamics of the Wadden Sea and its barrier island system. Ocean Coast Manag 68:39–57

Wright LD, Short AD (1984) Morphodynamic variability of surf zones and beaches: a synthesis. Mar Geol 56:93–118